JOURNAL OF Materials CHEMISTRY

Self-propagating high-temperature synthesis of ferrites MFe_2O_4 (M = Mg, Ba, Co, Ni, Cu, Zn); reactions in an external magnetic field

Warren B. Cross,[a] Louise Affleck,[a] Maxim V. Kuznetsov,[b] Ivan P. Parkin*[a] and Quentin A. Pankhurst[b]

[a]*Department of Chemistry, Christopher Ingold Laboratory, University College London, 20 Gordon Street, London, UK WC1H 0AJ*
[b]*Department of Physis and Astronomy, University College London, Gower Street, London, UK WC1E 6BT*

Received 3rd June 1999, Accepted 6th July 1999

Spinel ferrites of the form MFe_2O_4 (M = Mg, Co, Ni, Cu, Zn) and rhombohedral $BaFe_2O_4$ have been prepared by self-propagating high-temperature synthesis (SHS) reactions from iron, cobalt, iron(III) oxide and metal(II) oxides or peroxides. The driving force for the reactions is the oxidation of iron or cobalt powder. Reactions were carried out in air, under an oxygen atmosphere or with the addition of sodium perchlorate as an internal oxidising agent. Reactions were also carried out in the presence of an external magnetic field of 1.1 T. Pre-organisation of the reaction mixture in the applied field led to increases in the reaction velocity (from 2 to 5 mm s^{-1}) and temperature (950 to 1050 °C). The ratio of tetragonal to cubic phase observed for the $CuFe_2O_4$ product was increased by carrying out the reaction in the applied field. The inversion parameter observed for $MgFe_2O_4$ was also influenced by the applied field. All materials were characterised by X-ray powder diffraction (XRD), energy dispersive X-ray analysis (EDXA), scanning electron microscopy (SEM), FTIR, Mössbauer spectroscopy and vibrating sample magnetometry (VSM).

Self-propagating high-temperature synthesis (SHS) is a combustion technique that has been used to prepare a wide range of refractory materials.[1] We have recently shown that SHS is an ideal technique for the synthesis of representative hard[2] ($BaFe_{12}O_{19}$) and soft[3] ($Li_{0.5}Fe_{2.5}O_4$) ferrite materials. The SHS process is extremely rapid, producing ferrite materials in seconds, proceeding by a synthesis wave that moves through the precursors. The products after SHS require minimal treatment to produce single phase materials of high purity and figures of magnetic merit equivalent to commercially prepared materials.[4]

Ferrites are magnetic ceramic oxides having Fe_2O_3 as a major component. Hexagonal ferrites, such as $BaFe_{12}O_{19}$, are *hard* magnets having high coercivities and high saturation magnetisations. They are used as permanent magnets and in recording media where the material needs to be able to withstand demagnetizing forces.[5] Spinel ferrites are *soft* magnets having low coercivities, a property which along with their high resistivities leads to their application in microwave devices and transformers.[6] Generally the ferrites MFe_2O_4 have the metals in formal oxidation states of M^{II} and Fe^{III}. For the series of compounds where M is a Group 2 metal, only $MgFe_2O_4$ has a spinel type structure. $BaFe_2O_4$ (an intermediate in the SHS synthesis of $BaFe_{12}O_{19}$) has a complex structure similar to that of stuffed tridymite ($BaAl_2O_4$)[7] and $CaFe_2O_4$ has double rutile chains of FeO_6 octahedra enclosing eight-coordinate Ca.[8,9] A phase of composition $SrFe_2O_4$ has not been reported in the solid state phase diagram but has been prepared under harsh conditions.[10] Materials of formula MFe_2O_4 where M is Mn, Fe, Co, Ni, Cu or Zn are all of a spinel type structure.[5]

Ferrite materials are made by one of two major routes, either by a 'dry' traditional ceramic 'heat and beat' approach[5,11] or by a 'wet' co-precipitation[5,12] or sol–gel type[13] process. In the dry route, the precursors, normally metal oxides, are milled, fired and cooled repeatedly to form the final product. Particle sizes can be undesirably large, the materials are often inhomogeneous and the reaction times are long.[11] In the wet synthesis approach, dissolution of the metals in sulfuric acid, followed by precipitation with base, yields materials which on heating in air give homogeneous ferrites with small particle sizes[12] (< 1 μm). The sol–gel routes provide some of the best ferrite samples but are somewhat involved.[13] The synthesis technique used to prepare ferrite materials has a great influence on their magnetic and electrical properties. For example, the maximum magnitisation σ_{max} for the spinel ferrite $MgFe_2O_4$ varies between 18 and 30 emu g^{-1} dependent on the synthesis technique employed.[14] This variance is a consequence of the microstructure engendered by the different synthetic routes.

The spinel structure[5,15] is based around a face-centred cubic array of oxygen atoms with the cations filling either the tetrahedral (A) or octahedral (B) interstices within this array; there are 16 (out of 32) occupied octahedral sites and 8 (out of 64) occupied tetrahedral sites in the unit cell. Compounds of this type can have either a *normal* or *inverse* spinel structure. In a normal spinel the Fe^{3+} ions fill all the octahedral holes and the M^{2+} ions fill all the tetrahedral holes. For an inverse spinel, however, the tetrahedral sites are filled by half the Fe ions and the octahedral sites are filled by the other half of the Fe ions and all of the M^{2+} ions. The study of spinel chemistry, and in particular site occupation within spinels, has served as a classic text-book example of crystal field effects in solid state chemistry.[15]

There are two major influences on site occupancy in spinels: crystal field stabilisation energy (CFSE) and ionic radius. The radius of the tetrahedral site[5] is typically 0.5–0.67 Å and that of the octahedral site[5] typically 0.70–0.75 Å. Therefore, if an ion cannot be accommodated into the tetrahedral hole it will be located in the octahedral hole regardless of crystal field effects. Note that Ca^{2+} (radius 1.0 Å) and Ba^{2+} (1.35 Å) have too large a radius for either site.

For MFe_2O_4 where M belongs to the series Mn–Zn the ionic radius (comparable for all) has little influence on the structure, which is determined almost entirely by the CFSE of each cation

in each site. This is well illustrated by the site occupation in Fe_3O_4. Fe^{3+} has a CFSE of zero in both sites and so shows little site preference. Fe^{2+}, on the other hand, gives greater crystal field stabilisation when in the octahedral site. Thus, the structure of Fe_3O_4 is inverse: $(Fe^{3+})_A[Fe^{2+}Fe^{3+}]_BO_4$. Spinel ferrites can also have cation distributions between the extremes of normal and inverse. The site occupancy in these cases is quantified by the inversion parameter, x, in the representation $(M_{1-x}Fe_x)_A[M_xFe_{2-x}]_BO_4$; $x=0$ corresponds to the normal structure and $x=1$ the inverse structure.[6,15] The percentage inversion parameter in any ferrite system is typically determined by X-ray or Mössbauer techniques.

Here, we present the first synthesis of a range of spinel type ferrites by SHS reactions. In particular we have studied the effect of conducting the SHS reactions in the presence of an external magnetic field. The motivations for this study were to provide a new fast method of forming spinels, probe the change of inversion parameter under SHS conditions and to see whether an external magnetic field during SHS can influence ferrite magnetic and structural properties. This work is part of our wider study on the effects of an external magnetic field on reactions, especially on reactions that contain magnetic precursors.[2,3]

Experimental

All reagents were obtained from Aldrich Chemical Co. and used without further purification. Manipulations, weighing and grindings were performed under a nitrogen atmosphere in a Saffron Scientific glove box. Zero field SHS reactions were carried out in air with pre-ground powders on a ceramic tile or in a quartz tube under a flow of oxygen. Applied field SHS reactions were carried out in air or under a flow of oxygen, inside a quartz tube. The tube was inserted within a permanent Halbach cylinder magnet manufactured by Magnetic Solutions Ltd. The Halbach cylinder comprised eight NdFeB magnets which provided a field of 1.1 T along its length ($<2\%$ deviation in field along axis). Sintering was carried out on ground powders in a Carbolite rapid heating furnace with heating and cooling rates of 10 °C min^{-1}. Yields for the reactions were essentially quantitative, the only losses being mechanical. Powder X-ray diffraction (XRD) was performed on a Philips X-pert diffractometer using unfiltered Cu-Kα radiation in the reflection mode and on a Siemens D5000 using germanium monochromated Cu-Kα_1 ($\lambda=1.5406$ Å) radiation in the transmission mode. Lattice parameters were determined using the program Unit Cell. Scanning electron microscopy (SEM) and energy dispersive X-ray analysis (EDXA) were carried out with a Hitachi-S4000 instrument. Vibrating sample magnetometry (VSM) was carried out on an Aerosonic 3001 magnetometer at room temperature and at 80 K in applied fields up to 5 kOe. ^{57}Fe Mössbauer spectra were recorded with a Wissel MR-260 constant acceleration spectrometer with a triangular drive waveform. Spectra were folded to remove baseline curvature and were calibrated relative to α-Fe at room temperature. The spectra were fitted using a least squares fitting program. FTIR spectra were obtained on a Nicolet 205 spectrometer using pressed KBr disks. Synthesis wave temperatures were determined by optical pyrometry.

Zero magnetic field

Preparation of MFe_2O_4 (M = Mg, Ni, Cu, Zn). All of the MFe_2O_4 (M = Mg, Ni, Cu, Zn) materials were prepared in a similar manner illustrated below for M = Ni.

Nickel oxide (1.590 g, 21.3 mmol), iron powder (1.190 g, 21.3 mmol), Fe_2O_3 (1.530 g, 10.6 mmol) and $NaClO_4$ (0.980 g, 8.0 mmol) were ground together in a pestle and mortar. The green mixture was placed on a ceramic tile in air and a reaction initiated by a hot filament (800 °C). This induced an orange propagation wave of *ca.* 1–2 mm s^{-1} (*ca.* 950 °C). The products after SHS were ground, left in distilled water (*ca.* 250 cm^3) for 2 h, filtered under suction and washed with more water (*ca.* 1 dm^3). The resulting powder was oven dried (70 °C for 30 min) and sintered at 1150 °C for 2 h. Yield 4.21 g. Products were analysed by XRD, VSM, FTIR, SEM/EDXA and Mössbauer spectroscopy (Tables 1 and 2). Note for the preparation of $MgFe_2O_4$ the molar ratio of iron to iron oxide was increased from 2 : 1 to 4 : 1.

Preparation of $CoFe_2O_4$. Cobalt powder (1.26 g, 21.3 mmol), Fe_2O_3 (3.40 g, 21.3 mmol) and $NaClO_4$ (0.66 g, 5.33 mmol) were ground using a pestle and mortar and SHS reactions performed as for the other ferrites. The product was washed and oven dried as in the preparation of $NiFe_2O_4$ and sintered at 1150 °C for 2 h. The product was analysed by XRD, VSM, FTIR, SEM/EDXA and Mössbauer spectroscopy (Tables 1 and 2).

Preparation of $BaFe_2O_4$. Barium peroxide (2.653 g, 15.7 mmol), iron powder (0.922 g, 15.7 mmol) and Fe_2O_3 (91.298 g, 7.8 mmol) were ground using a pestle and mortar. A flow of oxygen was maintained over the reaction mixture and a synthesis wave initiated at one end of the powder with a hot filament. This produced a synthesis wave of velocity 2 mm s^{-1} (Fig. 1). The resulting black powder was sintered at 1150 °C for 2 h. The product was analysed by XRD, VSM, FTIR, SEM/EDXA and Mössbauer spectroscopy (Tables 1 and 2).

External magnetic field reactions

The same reactions were also studied by placing the green mixtures into a 0.8 cm i.d. quartz tube that was placed inside a Halbach cylinder magnet. It was noted that the whole of the green mixture was attracted into the centre of the magnetic field and adopted an hour-glass configuration with the long axis vertical (Fig. 2). The reactions inside the tube were initiated by a hot filament as before. The propagation velocity and synthesis wave temperatures were somewhat greater in the external magnetic field (*ca.* 5 mm s^{-1}, 1050 °C). The product obtained from the magnetic field experiments was removed by placing a plunger inside of the tube and forcing the contents

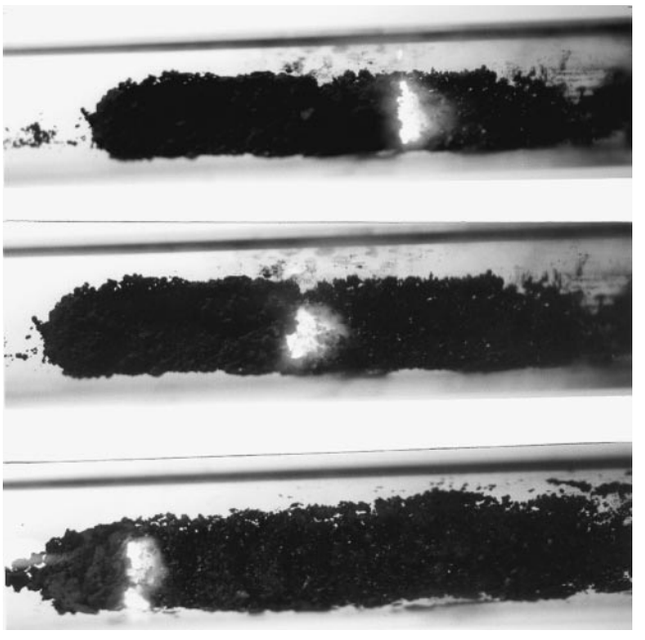

Fig. 1 Photographs of the SHS synthesis wave moving through a mixture of BaO_2, Fe and Fe_2O_3. The reaction was conducted inside a quartz tube (1 cm i.d.) and initiated by point source propagation on the right of the pictures. Propagation velocity was *ca.* 2 mm s^{-1}.

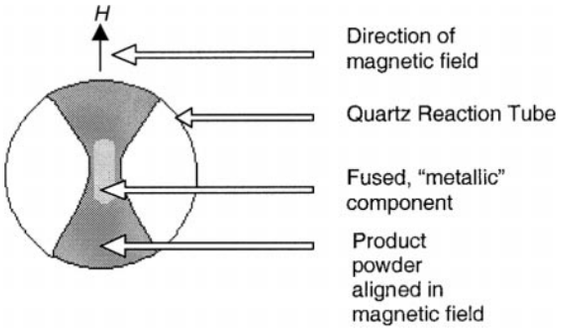

Fig. 2 Cross-section through the applied field SHS reaction tube. This figure shows the pre-alignment of the powders before SHS into an hour-glass shape and the position of the fused metallic looking component after the reaction.

out. Products were analysed by XRD, VSM, FTIR, SEM/EDXA and Mössbauer spectroscopy (Tables 1 and 2).

Caution: SHS reactions can be very exothermic, sometimes explosively, with any new system care should be taken to carry the reactions out behind a blast-proof screen. High temperature material can be ejected from the site of a laboratory scale reaction up to 1 m. Sodium perchlorate is a very strong oxidising agent which can react extremely violently with certain metal powders.

Results

Sample preparation

Ferrites of the form MFe_2O_4 (M = Mg, Co, Ni, Cu, Zn and Ba) were prepared by SHS reactions of metal powders and metal oxides on a ceramic tile or inside a quartz tube in an external magnetic field [eqn. (1)–(4)].

$$MgO + 1.25\ Fe + 0.375\ Fe_2O_3 + 0.9375\ O_2 \rightarrow MgFe_2O_4 \quad (1)$$

$$MO + Fe + 0.5\ Fe_2O_3 + 0.375\ NaClO_4 \rightarrow MFe_2O_4 + 0.375\ NaCl \quad (M = Ni, Cu, Zn) \quad (2)$$

$$Co + Fe_2O_3 + 0.25\ NaClO_4 \rightarrow CoFe_2O_4 + 0.25\ NaCl \quad (3)$$

$$BaO_2 + Fe + 0.5\ Fe_2O_3 + 0.25\ O_2 \rightarrow BaFe_2O_4 \quad (4)$$

Zero field reactions proceeded with an orange solid flame with a velocity of *ca.* 2 mm s^{-1} which spread out from the point of ignition (Fig. 1). Optical pyrometry indicated the reaction temperature to be *ca.* 950 °C. The products were dark grey or black powders except for $MgFe_2O_4$ (dark purple–grey) and $ZnFe_2O_4$ (orange–brown). These colours are in agreement with literature reports.[13–15]

The driving force for the reactions is the oxidation of an iron(0) or cobalt(0) metal fuel source to Fe(III) and Co(II) respectively (*ca.* 800 kJ mol^{-1}). The exothermicity of the reactions is sufficient to allow self-propagation. The iron(III) oxide added to the green mixture acts as moderator to ensure that the reaction is not unnecessarily exothermic. Sodium perchlorate acts as an intimately mixed source of oxygen for the reactions. On decomposition it produces oxygen gas, which oxidises the metal fuel source and drives the reaction, as well as sodium chloride. The sodium chloride melts at the reaction temperatures and probably acts as a wetting agent allowing the diffusion of other reacting ions and hence helping to propagate the SHS reaction by overcoming the solid state diffusion barrier.

The molar ratio of fuel (Fe) to moderator (Fe_2O_3) was chosen as 2 : 1 for all syntheses except for that of $MgFe_2O_4$. For this preparation a 2 : 1 ratio gave a material of mixed phases containing the desired product and unreacted precursors. Increasing the Fe to Fe_2O_3 ratio to 4 : 1 increased the exothermicity of the reaction, allowing isolation of single phase magnesium ferrite. The reaction to form $MgFe_2O_4$ did not employ sodium perchlorate but did use a flow of oxygen gas [eqn. (1)]. The reaction to form $BaFe_2O_4$ used barium peroxide as the internal oxidising source.

Enthalpy changes for the reactions [eqns. (1)–(4)] were calculated by Hess' Law, and determined to be between −275 and −400 kJ mol^{-1} [*e.g.* $\Delta_r H(CoFe_2O_4) = -275$ kJ mol^{-1}, $\Delta_r H(ZnFe_2O_4) = -382$ kJ mol^{-1}].[16] This is in agreement with empirical observations that indicate a value of *ca.* −300 kJ mol^{-1} is required for an SHS or SSM reaction to be self-sustaining.[17]

Reactions in an applied magnetic field typically showed faster propagation velocities of *ca.* 5 mm s^{-1} and higher reaction temperatures (1050 °C, as assessed by optical pyrometry). Furthermore, the physical appearance of the zero field (ZF) and applied field (AF) SHS products was notably different. When the reaction mixture was placed in the applied field, the presence of magnetic components in the powder (Fe, Fe_2O_3 or Co) meant that the whole reaction mixture (including the non-magnetic components) was drawn into and aligned by the external magnetic field, Fig. 2. In addition, after SHS, compounds prepared using an external field were more fused and the materials that were originally at the central part of field took on a metallic appearance.

Characterisation

X-Ray powder diffraction showed that single phase cubic spinel structures were produced for the sintered products MFe_2O_4, M = Mg, Co, Ni, Zn; a mixture of predominantly cubic $CuFe_2O_4$ with some tetragonal $CuFe_2O_4$ and rhombohedral $BaFe_2O_4$. Representative diffractograms are shown in Fig. 3, and the deduced lattice parameters are shown in Table 1. The indexed patterns gave cell constants that were equivalent to literature values.[18–22] The X-ray powder diffraction patterns of the ferrites directly after SHS and before washing with water and sintering, showed some multiphase products. The predominant phase was for the expected product MFe_2O_4, however NaCl was observed for reactions which employed $NaClO_4$ in the green mixture. Some traces of unreacted starting material were also noted in the initial products after SHS. These impurities were removed by washing with water and sintering. There was a small difference in the lattice parameter noted for the samples that were prepared by SHS in zero and an applied magnetic field of 1.1 T. This difference was not great enough to be statistically significant. The average crystallite size of the ferrite phase before sintering was *ca.* 200 Å and after sintering 300–500 Å as determined by the Scherrer equation.[23]

The FTIR spectra of the spinels were recorded as KBr discs in the range 4000–400 cm^{-1}. Spectra for the sintered materials showed two broad bands at 600–540 and 420–400 cm^{-1}.

Extensive work[24] on the vibrational spectra of spinels reveals two strong bands (ν_1 and ν_2) equivalent to those observed here and two less intense bands below 400 cm^{-1}. The two broad bands can be attributed to vibrations of bonds between the oxygen atoms and the highest valency cation.[24] Thus in this study both bands are due to vibrations of the 'FeO_6' and 'FeO_4' species. There was no relationship between the positions of the bands and the divalent metal cation, and both the zero field and applied field products gave the same spectra. The IR spectra of the unsintered products showed predominantly the ν_1 and ν_2 bands of the spinel structure. However, the unsintered products did show additional very weak intensity bands that could be attributed to unreacted starting material.

EDXA measurements of the 'as made' zero-field ferrites after trituration with water but prior to sintering showed regions with homogeneous elemental distributions with the expected 1 : 2 elemental ratio of M : Fe (oxygen was below the machine

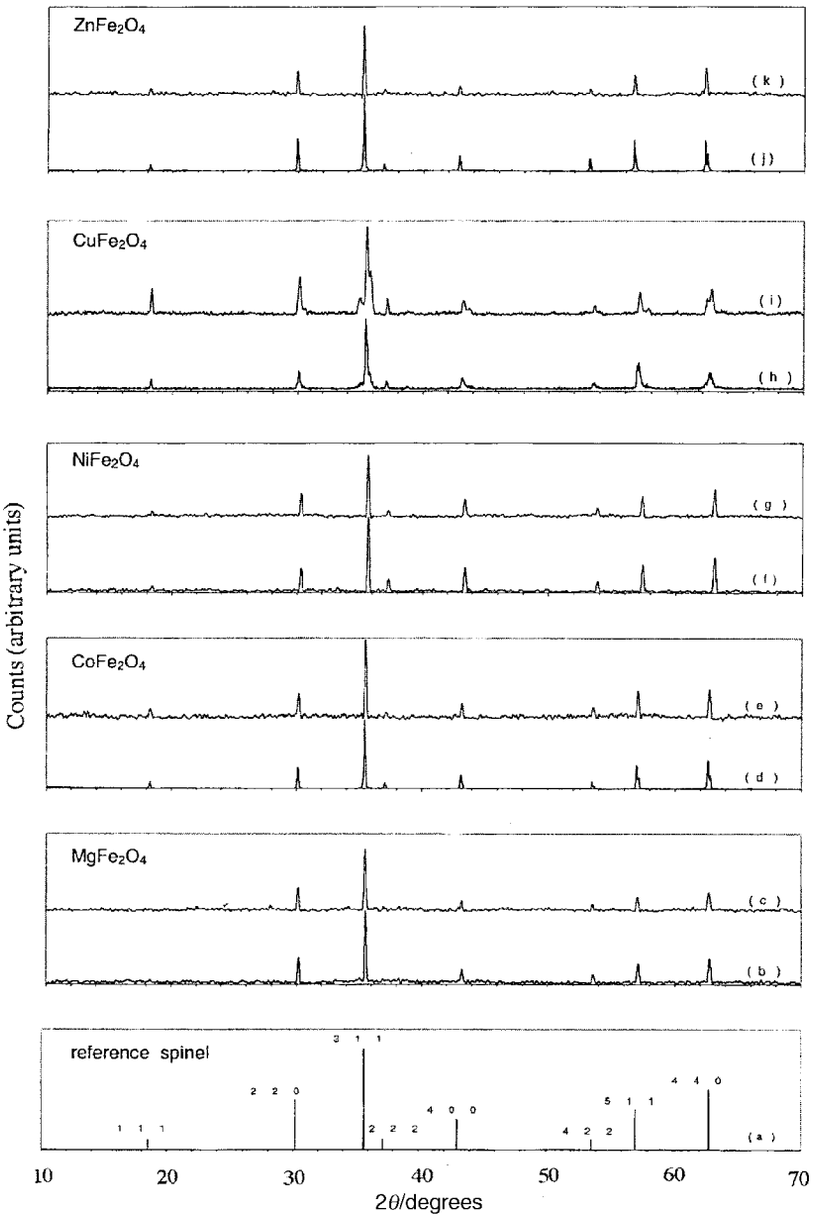

Fig. 3 X-Ray powder diffraction patterns for (a) reference spinel; (b) $MgFe_2O_4$-ZF; (c) $MgFe_2O_4$-AF; (d) $CoFe_2O_4$-ZF; (e) $CoFe_2O_4$-AF; (f) $NiFe_2O_4$-ZF; (g) $NiFe_2O_4$-AF; (h) $CuFe_2O_4$-ZF; (i) $CuFe_2O_4$-AF; (j) $ZnFe_2O_4$-ZF; (k) $ZnFe_2O_4$-AF, products obtained from SHS reactions after sintering at 1150 °C for 2 h. Note (d), (h) and (j) were measured on a Philips diffractometer with no filtering of the radiation. Hence α_1 and α_2 line splittings are seen at high angle.

cut-off) over many surface spots. However some inhomogeneity was noted, consistent with unreacted starting material. SEM analysis of the products revealed agglomerates of particles of size *ca.* 1 μm. The samples prepared in an external magnetic field were more homogeneous. This is probably a consequence of the higher reaction temperatures in the applied field synthesis giving rise to a more complete reaction. After sintering, the inhomogenity noted in the zero field samples disappeared.

Mössbauer spectra were recorded at room temperature for

Table 1 X-Ray powder diffraction data of the zero field (ZF) and applied field (AF) products prepared by SHS after sintering at 1150 °C for 2 h

Reaction[a]	Phase identified by XRD	Lattice parameters/ Å (Zero field)	Lattice parameters/ Å (Applied field)	Literature lattice parameters
$MgO+Fe+Fe_2O_3$	Cubic $MgFe_2O_4$	$a=8.3639(7)$	$a=8.3674(3)$	$a=8.367(2)$
$Co+Fe_2O_3+NaClO_4$	Cubic $CoFe_2O_4$	$a=8.3385(2)$	$a=8.3894(7)$	$a=8.394(5)$
$NiO+Fe+Fe_2O_3+NaClO_4$	Cubic $NiFe_2O_4$	$a=8.331(1)$	$a=8.3335(8)$	$a=8.339(5)$
$CuO+Fe+Fe_2O_3+NaClO_4$	Cubic $CuFe_2O_4$	$a=8.393(2)$	$a=8.372(2)$	$a=8.380(4)$
	Tetragonal $CuFe_2O_4$[b]			
$ZnO+Fe+Fe_2O_3+NaClO_4$	Cubic $ZnFe_2O_4$	$a=8.437(2)$	$a=8.430(5)$	$a=8.440(2)$
$BaO_2+Fe+Fe_2O_3$	Rhombohedral $BaFe_2O_4$	$a=19.04(1)$	$a=19.04(1)$	$a=19.05(1)$
		$b=5.367(5)$	$b=5.385(3)$	$b=5.385(3)$
		$c=8.42(2)$	$c=8.43(2)$	$c=8.448(6)$

[a]The initial stoichiometry of the reagents used in the reaction is detailed in the experimental section and eqn. (1)–(4). [b]The tetragonal phase was a minor component and was not indexed.

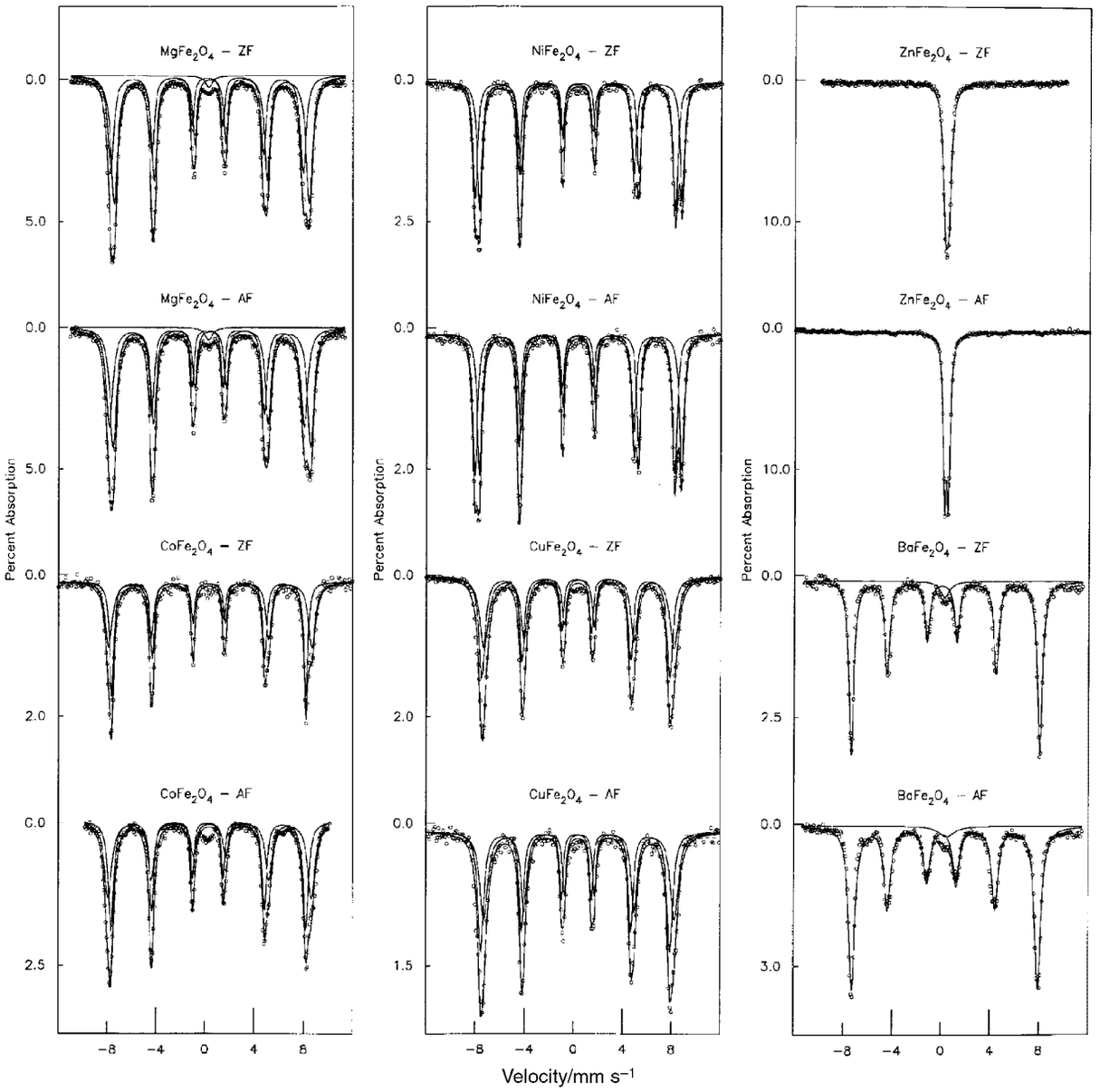

Fig. 4 Room temperature Mössbauer spectra for the spinel ferrites derived from SHS reactions in zero field and an external field of 1.1 T, after sintering at 1150 °C for 2 h. Solid lines represent a least squares fit with two subcomponents corresponding to the Fe atoms in octahedral and tetrahedral sites.

all the ferrites, Fig. 4. The spectra were least squares fitted using Lorentzian lineshapes and a first order perturbation approach to the combination of electric quadrupole and magnetic interactions. Data points are shown in the spectra as crosses, with fitted spectra as solid lines. Mössbauer parameters derived from the spectra are shown in Table 2.

Table 2 Mössbauer and magnetic data on the spinel ferrites prepared by zero field (ZF) and applied field (AF) SHS after sintering at 1150 °C for 2 h[a]

Spinel	δ	Δ	Γ	B_{hf}	δ	Δ	Γ	B_{hf}	σ_{max}/emu g^{-1}	σ_r/emu g^{-1}	H_c/Oe	Lit. σ_{max}/emu g^{-1}
$MgFe_2O_4$–ZF	0.43	0.05	0.52	492	0.12	−0.09	0.46	485	19	5	40	18–30
$MgFe_2O_4$–AF	0.46	0.06	0.53	498	0.14	−0.12	0.50	491	19	5	40	18–30
$CoFe_2O_4$–ZF	0.37	0.02	0.52	512	0.26	−0.01	0.38	489	71	15	430	65–80
$CoFe_2O_4$–AF	0.38	−0.04	0.64	512	0.26	−0.01	0.41	491	72	19	440	65–80
$NiFe_2O_4$–ZF	0.48	−0.01	0.36	521	0.26	0.01	0.43	492	47	14	75	40–50
$NiFe_2O_4$–AF	0.36	−0.02	0.37	520	0.25	0.00	0.41	492	49	10	75	40–50
$CuFe_2O_4$–ZF	0.44	0.01	0.61	479	0.21	−0.03	0.46	474	44	9	70	30–42
$CuFe_2O_4$–AF	0.48	0.01	0.57	481	0.22	−0.05	0.45	477	42	10	65	30–42
$ZnFe_2O_4$–ZF	0.34	0.29	0.45						2	0.6	100	0
$ZnFe_2O_4$–AF	0.35	0.33	0.31						4	0.6	80	0
$BaFe_2O_4$–ZF	0.19	0.32	0.48	477					1.2	0.8	2200	
$BaFe_2O_4$–ZF	0.19	0.31	0.63	471					2.4	1.7	2100	

[a]Cobalt, nickel and copper ferrites were modelled with equal area sextets. Magnesium ferrite was fitted with a B : A site area ratio of $1:0.67\pm0.03$ (ZF SHS) and $1:0.84\pm0.05$ (AF SHS). Isomer shift ($\delta\pm0.01$ mm s^{-1}), quadrupole shift ($\Delta\pm0.02$ mm s^{-1}), linewidth ($\Gamma\pm0.001$ mm s^{-1}) and hyperfine field ($B_{hf}\pm1$ kOe) are given for the octahedral B-site sextet in the first four columns in the table and for the tetrahedral A-site in the next four columns. The zinc ferrite material showed a Mössbauer doublet; $BaFe_2O_4$ was modelled as a single sextet.

The Mössbauer spectra for $MgFe_2O_4$, $CoFe_2O_4$, $NiFe_2O_4$ and $CuFe_2O_4$ were fitted with two subcomponents, both sextets corresponding to Fe(III) in magnetic sites. These materials have the inverse spinel structure, unlike zinc ferrite which is a normal spinel. Thus, each sextet corresponds to Fe^{3+} in either the A (tetrahedral) or B (octahedral) sites within the fcc array of oxygen atoms. The sextet with the lower isomer shift (δ) and smaller hyperfine splitting (B_{hf}) represents the A site, and the sextet with the highest isomer shift and largest hyperfine splitting represents the B site. In all cases the quadrupolar splitting is close to zero.

The areas of the two sextets represent the site occupation of the spinel. The site occupation is quantified by the inversion parameter, x, in the representation: $(M_{1-x}Fe_x)_A[M_xFe_{2-x}]_BO_4$. ($x=0$, normal; $x=1$, inverse). For cobalt and copper ferrite the ratio of the areas had to be constrained to 1 : 1 during the fitting because the two sextets overlapped to a great extent. However, literature reports indicate that the ratio should be 1 : 1, or very close this value, and constraining the ratio gives a very good fit in each case ($\chi^2=1.4$, 2.8). When fitting $NiFe_2O_4$ the areas could be varied, since the sextets are well separated, but the best fit was still obtained with the areas in a 1 : 1 ratio [$\chi^2=2.4$ for zero field (ZF) SHS and 1.6 for applied field (AF) SHS spectrum]. Thus, cobalt, nickel and copper spinel ferrites prepared by SHS have an inversion parameter $x=1$, *i.e.* $(Fe^{3+})_A[M^{2+}Fe^{3+}]_BO_4$.

It is known that magnesium ferrite deviates from $x=1$ and the cation distribution depends markedly upon the method of synthesis.[11–13,22] Allowing the areas of the two sextets to vary relative to each other gives a value of $x=0.80$ for $MgFe_2O_4$ prepared by SHS in the absence of a magnetic field, and $x=0.92$ when prepared in the presence of an external field. These values are common for this compound,[18] but the change is quite dramatic considering that the only difference between the two materials is that one was synthesised within an applied field and one in zero field. The Mössbauer spectrum of magnesium ferrite shows a small (relative area 2.5%) doublet as well as two sextets. This additional peak is probably not due to impurities, as none were observed by EDXA or in the X-ray diffraction pattern, but it is more likely to be due to paramagnetic or super-paramagnetic $MgFe_2O_4$ clusters. This phenomenon has been observed before for conventionally prepared materials.[18,25]

Two sextets are observed in the Mössbauer spectra of the inverse spinels because there are two environments for iron (A and B sites) both of which are magnetic due to antiferromagnetic coupling between the two sites. In a normal spinel ferrite all the Fe^{3+} cations are found on the B sites, which are non-magnetic if the cations on the A site are non-magnetic (antiferromagnetic superexchange is zero). Therefore, the Mössbauer spectrum of $ZnFe_2O_4$ is a single doublet corresponding to the single paramagnetic environment of Fe^{3+} in the normal spinel $(Zn)_A[Fe_2]_BO_4$. There is no evidence in the spectrum to suggest that iron(III) cations are found in other environments, and hence no partial inversion is observed for this material.

Hysteresis loops were recorded for the SHS derived ferrites up to 5 kOe at room temperature, Fig. 5, and data corrected for sample geometry compared to nickel powder. The maximum magnetisation (σ_{max}), remanent magnetisation (σ_r) and coercivity (H_c) are presented in Table 2 and compared with literature values.[5,18,24] The magnetic properties all fall within the range reported in the literature. Such a spread exists in the literature because the properties of these materials strongly depend upon the method used for synthesis.[14] All of the materials were soft magnets with relatively high saturation magnetisations, low coercivities and minimal hysteresis. A hysteresis loop has been recorded for zinc ferrite, even though the Mössbauer spectra for this material suggested that it is paramagnetic at room temperature. Whereas the inverse spinels have high magnetisations due to strong antiferromagnetic coupling between Fe^{3+} on A and B sites (A–B superexchange), the normal spinel $ZnFe_2O_4$ only has magnetic Fe^{3+} cations on the B sites, so cannot undergo this strong A–B coupling. It is therefore suggested that hysteresis behaviour is observed in this paramagnetic material due to weak B–B interactions, giving low magnetisation. No significant changes in magnetic parameters were observed between samples prepared in zero or an applied magnetic field.

Discussion

The X-ray diffraction pattern for $CuFe_2O_4$ synthesised by ZF SHS shows very small amounts of a phase which is not the cubic spinel (Fig. 5). If the SHS reaction is carried out in an external magnetic field, however, these extra peaks are much larger. These extra peaks in the diffraction pattern correspond to tetragonal $CuFe_2O_4$. Thus, two phases are observed with the same stoichiometry, with the AF SHS reaction giving a greater proportion of the tetragonal phase. Copper ferrite is a somewhat unique example of a simple spinel which undergoes tetragonal distortion. $CuFe_2O_4$ is an inverse spinel, Fe^{3+} cations occupy the tetrahedral and half the octahedral sites, whereas the Cu^{2+} cations occupy the remaining half of the octahedral sites. Copper(II) is also a Jahn–Teller ion and can distort to give a tetragonal crystal system.

This polymorphism has been shown to occur many times in copper ferrite systems: for example ball-milling a material of the tetragonal phase for 98 h has lead to an entirely cubic phase material.[24] Perhaps more relevant to this study, is the fact that the synthesis temperature has been determined to affect the phase of the copper ferrite prepared.[26] Combustion synthesis of $CuFe_2O_4$ from metal nitrates gave a material which was then sintered at a range of temperatures. Low temperature sintering gave the cubic spinel phase, whereas high temperature sintering gave entirely the tetragonal phase product.

We have previously suggested that pre-alignment of the reaction mixture in an external magnetic field creates lines of fuel along which the reaction proceeds at faster velocities and higher temperatures.[2,3] This suggestion supports the results presented here which show a greater proportion of the (higher temperature) tetragonal phase copper ferrite formed in the AF SHS reaction. It also ties in with the faster propagation velocity and the higher synthesis wave temperatures observed in the applied magnetic field. It was also interesting to note that the starting precursor powders including the non-magnetic components were sucked into the magnetic field and that they aligned themselves in correlation with the magnetic field axis. The fact that the particles were preground prior to SHS probably meant that the non-magnetic components were coated in sufficient magnetic iron or cobalt metal to ensure that all of the material was drawn into the magnetic field. After the passage of the SHS synthesis wave the material had darkened in colour and the central portion of the product (*ca.* 5–10%) appeared metallic and fused in appearance. This metallic component is of the same composition by EDAX as the rest of the product (*i.e.* no enhancement in iron or cobalt). Further work is underway to determine the extent of metallic formation in other ferrite systems and to investigate the product microstructure in detail.

Previous work on the formation of hard magnetic materials such as $BaFe_{12}O_{19}$ by SHS in an external magnetic field produced materials with greatly different magnetic properties compared to materials synthesised by SHS in zero field.[2] For example, barium ferrite synthesised in an external field showed approximately half of the coercivity of materials synthesised in the absence of a field.[2] Such large changes in

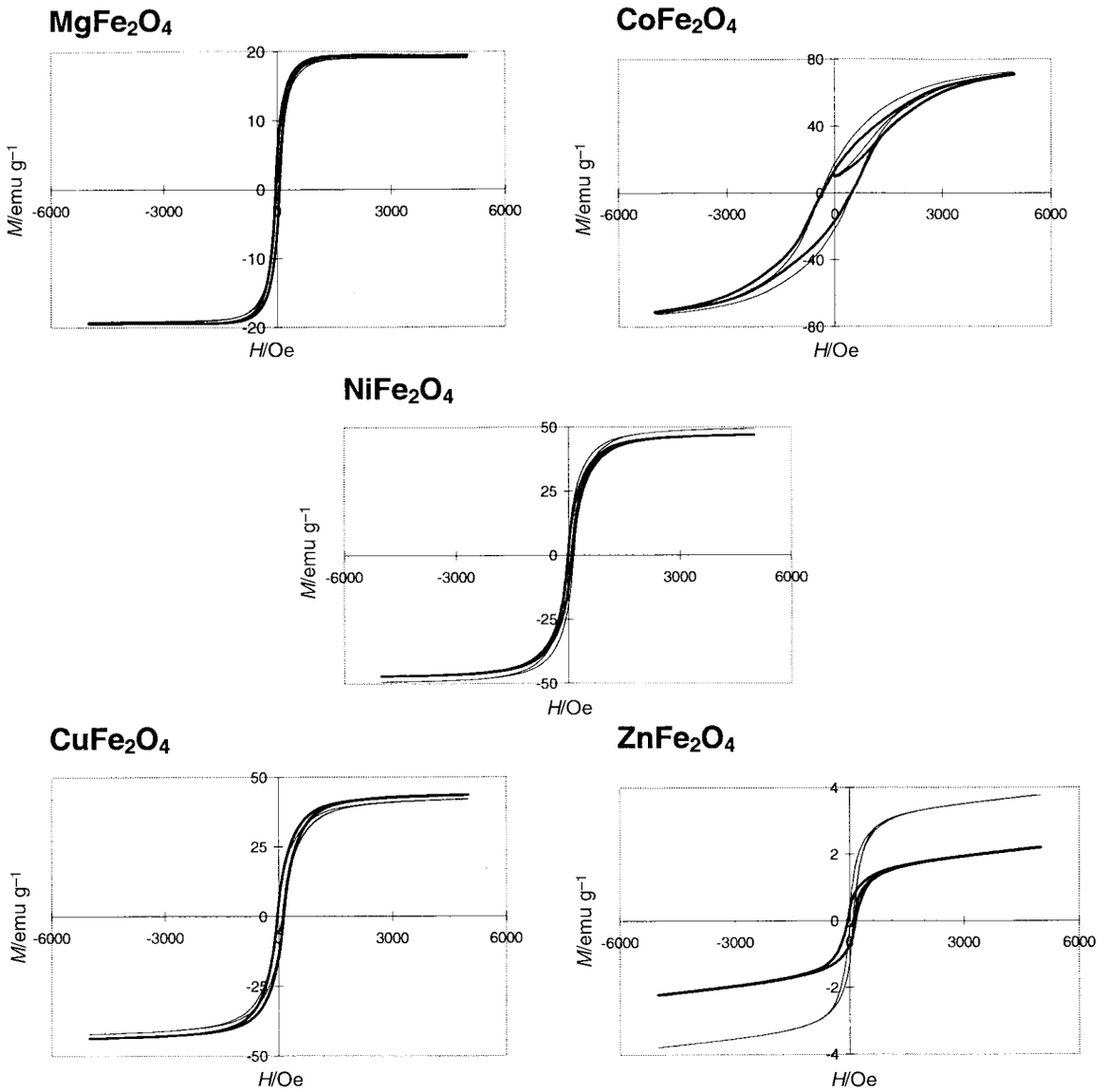

Fig. 5 Representative hysteresis loops for the spinel ferrites prepared in zero field (ZF) and in an applied field (AF) of 1.1 T after sintering at 1150 °C for 2 h. The darker lines on the hysteresis loops represent the ZF measurements.

magnetic figures of merit were not observed for the formation of spinel ferrites by SHS. Notably, for both the zero field and applied field synthesis of ferrites by SHS the products obtained showed σ_{max} at the highest end of the literature values (except for $MgFe_2O_4$).

One reason for studying the formation of spinel ferrite systems is the limited number of crystallographic sites available for substitution chemistry. Previously for hard magnetic systems ($BaFe_{12}O_{19}$) we suggested that the changes in magnetic properties were due to either changes in product microstructure or site occupancy. In the spinel systems reported here, it appears that in the majority of cases the site occupancy of the spinels is not altered by performing a reaction in a magnetic field and the high magnetisation values reported are an effect of a fine grained product microstructure. In the case of magnesium ferrite the applied field did have some effect on the inversion parameter. This is most easily explained by the effect of the field organising the starting reaction mixture. In the zero field reactions $x=0.80$ for $MgFe_2O_4$ compared to $x=0.92$ when prepared in the presence of an applied field. This change of inversion parameter is small but significant. It is probably a reflection of the fact that in the applied magnetic field the reaction is at a slightly higher temperature. Values of the inversion parameter in the range 0.75–1.00 have been reported previously for magnesium ferrite.

Conclusions

SHS offers a fast method for the synthesis of spinel type ferrites with equivalent physical properties to conventional preparations. The ferrites were made from reaction of metal, metal oxide and sodium perchlorate powders. The reactions proceed in air *via* a propagation wave of temperature 950 °C and velocity 2 mm s^{-1}. In the presence of a 1.1 T external magnetic field the reaction proceeded at higher temperature (*ca.* 1050 °C) and with faster propagation velocity (5 mm s^{-1}). This was attributed to arrangement of the starting magnetic powders within the external field such that the Fe or Co fuel source aligned along field lines giving an easy pathway for reaction propagation. Differences were observed between the zero field and applied field reactions. In an applied field the $CuFe_2O_4$ product showed more tetragonal component. The cation distribution in $MgFe_2O_4$ showed an inversion parameter of $x=0.92$ for the applied field reactions and $x=0.80$ for the zero field reactions.

Acknowledgements

The Mössbauer spectra were obtained under the auspices of the ULIRS Mössbauer service. M.V.K. thanks the Royal Society for a travel grant.

References

1 A. G. Merzhanov, *Adv. Mater.*, 1992, **4**, 294; *Int. J. Self-Propag. High-Temp. Synth.*, 1995, **4**, 323; Q. A. Pankhurst and I. P. Parkin, *Mater. World*, 1998, 743.
2 M. V. Kuznetsov, Q. A. Pankhurst and I. P. Parkin, *J. Mater. Chem.*, 1998, **8**, 2701; I. P. Parkin, G. E. Elwin, A. V. Komarov, Q. T. Bui, Q. A. Pankhurst, L. Fernandez Barquin and Y. G. Morozov, *J. Mater. Chem.*, 1996, **6**, 199.
3 I. P. Parkin, M. V. Kuznetsov and Q. A. Pankhurst, *J. Mater., Chem.*, 1999, **9**, 273; M. V. Kuznetsov, Q. A. Pankhurst and I. P. Parkin, *J. Phys. D*, 1998, **31**, 2886.
4 I. P. Parkin, G. E. Elwin, A. V. Komarov, Q. T. Bui, Q. A. Pankhurst, L. Fernandez Barquin and Y. G. Morozov, *Adv. Mater.*, 1997, **9**, 643.
5 J. Smit and H. P. J. Wijn, *Ferrites*, Wiley, New York, 1959.
6 E. C. Snelling, *Soft Ferrites*, Butterworths, London 2nd edn., 1988.
7 H. Mitsuda, S. Mori and C. Okazaki, *Acta Crystallogr., Sect. B*, 1971, **27**, 1263.
8 P. M. Hill, H. S. Peiser and J. R. Rait, *Acta Crystallogr.*, 1956, **9**, 81.
9 B. F. Decker and J. S. Casper, *Acta Crystallogr.*, 1957, **10**, 332.
10 P. Berthet, J. Berthon, G. Hegger and A. Revolevschi, *Mater. Res. Bull.*, 1992, **27**, 919.
11 D. A. Rawlinson, Ph.D. Thesis, Brunel University, 1998.
12 A. Goldman and A. M. Laing, *J. Phys.*, 1976, **4**, C1.
13 J. Livage, M. Henry and C. Sanchez, *Prog. Solid State Chem.*, 1988, **18**, 259; A. Chatterjee, D. Das, S. K. Pradhan and D. Chakravorty, *J. Magn. Magn. Mater.*, 1993, **127**, 214.
14 G. Economos, *J. Am. Ceram. Soc.*, 1955, **38**, 335; G. A. Swanski, F. van der Woude and A. H. Morrish, *Phys. Rev.*, 1968, **187**, 747; E. de Grave, A. Govaert, D. Chambaere and G. Robbrecht, *Physica B*, 1979, **96**, 103.
15 J. P. Jakubovics, *Magnetism and Magnetic Materials*, Cambridge University Press, 2nd edn., 1994, p. 38; S. Krupicka and P. Novak, *Ferromagnetic Materials*, ed. E. P. Wohlfarth, 1982, vol. 3, p. 189.
16 D. D. Waymann, W. H. Evans, V. B. Parker, R. H. Schuum, I. Harlow, S. M. Bailey, H. C. Chumey and R. L. Nuttal, *The NBS Tables of Chemical and Thermodynamic Properties*, American Chemical Society, Washington DC, 1982.
17 I. P. Parkin, *Chem. Soc. Rev.*, 1996, 199; I. P. Parkin, L. Affleck, M. D. Aguas, W. Cross, M. V. Kuznetsov, Q. A. Pankhurst and A. Steer, *Am. Chem. Soc. Div. Inorg. Chem. Abstr.*, 1999, 527.
18 H. St. C. O'Neill, *Eur. J. Mineral.*, 1992, **4**, 571.
19 J. G. Na, T. D. Lee, E. C. Kim and S. J. Park, *J. Mater. Sci. Lett.*, 1993, **12**, 361.
20 Landolt-Börnstein, *Numerical Data and Functional Relationships in Science and Technology*, Springer-Verlag, New York, 1970, vol. III 4b.
21 G. F. Goya, H. R. Rechenberg and J. Z. Jiang, *J. Appl. Phys.*, 1998, **84**, 1101.
22 R. G. Kulkarni and H. H. Joshi, *J. Solid State Chem.*, 1986, **64**, 141.
23 H. P. Klug and L. E. Alexander, *X-Ray Diffraction Procedure for Polycrystalline and Amorphous Materials*, Wiley, New York, 2nd edn., 1974.
24 J. Preudhomme and P. Tarte, *Spectrochim. Acta, Part A*, 1971, **27**, 1817; 1972, **28**, 69.
25 Z. Gao, T. Wu and S. Peng, *J. Mater. Sci. Lett.*, 1994, **13**, 1715.
26 Y. Zhang and G. C. Stangle, *J. Mater. Res.*, 1994, **9**, 1997.

Paper 9/04431K